Semi-quantitative analysis of geological samples using laser plasma time-of-flight mass spectrometry

Qingguo Tong,[a] Quan Yu,[a] Xianzhong Jin,[a] Jian He,[b] Wei Hang[*ab] and Benli Huang[a]

A method has been developed that allows the direct measurement of the elemental composition of geological samples based on a newly developed laser plasma time-of-flight mass spectrometer with a collisional cooling system. This technique has the merits of small sample consumption and rapid elemental analysis. Four geological reference materials were used in the experiment. The system has shown a satisfactory resolving power with few interferences in the spectra. The limits of detection were about 10^{-6}–10^{-7} g g^{-1} for most of the metal elements. The relative sensitivity coefficients (RSCs) of the elements with mass heavier than 30 amu could be used for direct semi-quantitative analysis.

Introduction

The determination of metals in geological materials is of major importance in geoanalysis. Conventionally, geological samples are analyzed by a variety of analytical techniques after cumbersome preparation and decomposition procedures.[1] As the number of samples and elements to be analyzed grows, the complexity of the sample preparation step overshadows that of the actual analytical measurements.

Laser ablation is considered one of the most versatile techniques for the analysis of solid samples.[2] Focusing a short-pulse, high-fluence laser beam onto a sample surface will create an explosion that produces ions, atoms, clusters and particles[3] for direct analysis by optical or mass spectrometry, or introduction into an ICP-MS. Currently, the prevalent laser ablation technology for solid sampling is inductively coupled plasma mass spectrometry (LA-ICP-MS). Fundamentally, LA-ICP-MS has been applied to the element- and isotope-specific analysis of different types of solid materials,[4–7] mainly due to its great experimental flexibility and lack of restrictions to the sample shape, size, or nature. Although its advantages are known, it suffers from large consumption of inert gas and memory effects. Moreover, due to the gas species interference and elemental fractionation effects, suitable reference standards and non-linear calibrations are routinely necessary for quantitative analysis.[8] Nevertheless, LA-ICP-MS plays a dominant role in the direct elemental analysis of solids.

Previous utilization of a laser beam to vaporize and excite atoms from solid targets was started by Honig et al. in the 1960s.[9] In subsequent years, laser ionization (LIMS),[10] the laser microprobe mass analyzer (LAMMA)[11] and other laser-related direct solid analytical techniques have been used extensively and proved to be very useful qualitatively with a typical sensitivity of 10^{-6} g g^{-1}. However those instruments used a laser irradiance $< 10^9$ W cm^{-2} for atomization and ionization, which led to significant differences in elemental sensitivity, and if a laser irradiance $> 10^9$ W cm^{-2} were applied, the spectral resolution would have been too poor for any analytical purpose.

Like LA-ICP-MS, our newly constructed laser plasma time-of-flight mass spectrometer (LP-TOFMS) has the advantage of simple sample preparation. The instrument employs a collisional cooling multipole device to reduce the kinetic energy distribution of ions generated in laser plasma with an irradiance $> 10^9$ W cm^{-2}. Consequently, the LP-TOFMS provides simultaneous multielemental detection with good resolution. In this article, we present the approach for the direct analysis of metal elements in geological samples based on the LP-TOFMS.

Experimental

Instrument

The in-house-built instrument consists of a pulsed laser source, a collisional cooling cell, an orthogonal time-of-flight mass spectrometer, and a recording system for data collection and integrating sequential spectra. The schematic diagram of the system is shown in Fig. 1. The instrumentation has been previously described by Peng et al.,[12] but the transmission system was modified and improved.

A 532 nm wavelength, 4.4 ns pulse width Nd:YAG laser (NL303G, EKSPLA) was used for ablation and ionization. The focused laser spot was 40 μm in diameter and surveyed by a metallographic microscope. The typical laser irradiation flux was 2×10^{10} W cm^{-2}, and the laser frequency was set at 10 Hz. A laser power meter was utilized to monitor the energy of the laser pulses after the iris (5.5 mm in diameter). The ion source formed the first vacuum stage, in which the pressure was maintained at several hundred Pa during the experiment. Ultra-high purity helium (99.999%) was used as the buffer gas.

The disc sample was mounted onto a home-made direct insertion probe (DIP) with no voltage applied (floated). The DIP was rotated manually after every 100 laser shots on the same spot. In our previous work,[12] a small hexapole was located between the nozzle and skimmer 1 to transmit ions and reduce

[a] Department of Chemistry, College of Chemistry and Chemical Engineering, The Key Laboratory of Analytical Sciences of the Ministry of Education, Xiamen University, Xiamen, 361005, China. E-mail: weihang@xmu.edu.cn
[b] Department of Mechanical and Electrical Engineering, Xiamen University, Xiamen, 361005, China
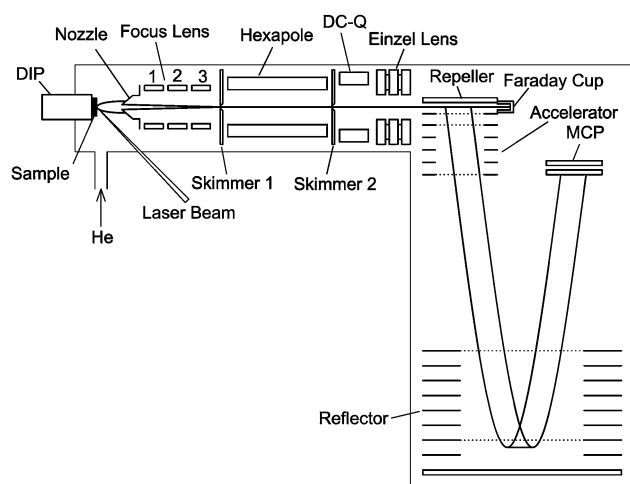
Fig. 1 Schematic diagram of the laser plasma time-of-flight mass spectrometer.

the radiation of the ion beam. However, mass discrimination was found due to the transmission property of the hexapole. Currently, three stainless steel cylindrical lenses have been introduced to replace the small hexapole. With this change, the problem of suppressed signals of small ions could be alleviated to some extent. After skimmer 1, a home-made rf-only hexapole system was employed for transmission and cooling of the ions.

The mass analyzer was a home-made TOF with an angular reflectron. TOF mass spectra were recorded by a single channel time-to-digital converter (TDC, Ionwerks) with a time resolution of 0.625 ns. A preamplifier (Model 6954, Phillips Scientific) and constant fractional discriminator (935 Quad CFD, Ortec) were used before the TDC. Due to the air leaking to the source chamber during sample loading, the laser was triggered about 5 minutes after sample loading to get a clean spectrum. Spectra were acquired by accumulating signals for 10 min. The detailed operating conditions are listed in Table 1.
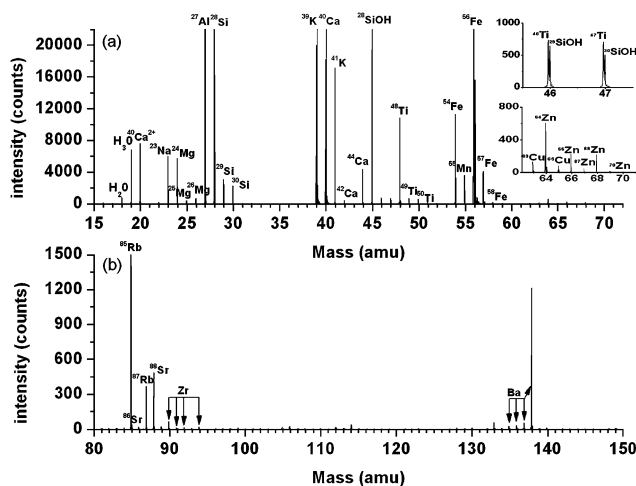
Sample preparation

A 0.1 g powdered geological sample was loaded into a die and pressed with 5×10^7 Pa of pressure for 5 min by a hydraulic press machine. After preparation, the sample had the form of a tablet with a thickness of 1.5 mm and diameter of 6 mm. Four reference powdered materials were prepared to disc shape and analyzed using the LP-TOFMS: GBW(E)070041, GBW(E)070043,

Table 1 Typical operating parameters

Laser incident angle	45°
Focus lens 1	118.5 V
Focus lens 2	85.5 V
Focus lens 3	51 V
Nozzle	1.5 mm orifice, 154.5 V
Skimmer 1	1.0 mm orifice, −5.5 V
TOFMS pressure	8.7×10^{-5} Pa
Repelling frequency	16.7 kHz
Repelling pulse magnitude	745 V
Acceleration potential	−4848 V
CFD threshold levels	−120 mV

GBW(E)070045 (Soil standards, Institute of Soil Science, Chinese Academy of Sciences), and YSS030-2006 (Zinc concentrate, Huludao Yongsheng non-ferrous Metals Trading Ltd., China).

Results and discussion

Laser ablation and ionization of solids is a complex process that depends on the laser parameters (irradiance, wavelength, pulse width and the beam profile) and also on the physical and chemical properties of the various components present in the sample (morphology, homogeneity, absorption properties and surface orientation).[13,14] The determination of the elemental composition of geological samples requires careful control of operating parameters and choice of optimal conditions. A laser irradiation flux of 10^9–10^{10} W cm^{-2} is a preferable laser power for the elemental analysis of solids because there is little fractional evaporation in this laser irradiance range.[10,15] In our system, ion intensities from the source chamber were mainly affected by the laser irradiance, distance from sample to nozzle, and pressure of the buffer gas. After the optimization, a laser irradiance of 2×10^{10} W cm^{-2}, a helium pressure of 360 Pa, and a distance of 5 mm from the sample to the nozzle were chosen for achieving high singly charged ion intensity, suppressing the multiply charged and gas species interferences, and compromising the light and heavy ion sampling.

A typical spectrum of GBW(E)070043 is shown in Fig. 2. The similar spectra of GBW(E)070041 and GBW(E)070045 are omitted. As indicated in Fig. 2, the major interferences were at m/z 18 (H_2O^+) and 19 (H_3O^+). The appearance of H_2O^+ and H_3O^+ might be caused by the residue gas in the source chamber and impurities in the helium gas. The peak of silicon hydroxide [$(SiOH)^+$] was found since silicon was easier to combine with oxygen because of the higher enthalpy of formation ($\Delta H_f = 798$ kJ mol^{-1} for SiO^+). However, with the collisional cooling device and orthogonal geometry, the system can achieve a high resolving power to resolve signals from interferences. As seen in Fig. 2, ^{46}Ti and ^{47}Ti peaks can be resolved with ^{29}SiOH and ^{30}SiOH interferences. All major and minor elements are clearly shown in the spectrum. Peaks representing Rb, Sr, Zr and Ba,

Fig. 2 Mass spectrum of GBW(E)070043.

Table 2 RSCs of different elements in GBW(E)070041, GBW(E)070043 and GBW(E)070045; LODs of different elements in GBW(E)070043 (^{55}Mn as reference element)

Element (isotope used)	Concentration of GBW(E) 070041/μg g^{-1}	RSC	Concentration of GBW(E) 070045/μg g^{-1}	RSC	Concentration of GBW(E) 070043/μg g^{-1}	RSC	LODs/μg g^{-1}
^{23}Na	18 400	0.03	670	0.05	7300	0.08	1.39
^{24}Mg	7663	0.06	2560	0.05	9875	0.06	2.10
^{27}Al	79 700	0.02	77 200	0.04	78 000	0.05	2.49
^{29}Si	281 210	0.01	301 494	0.02	231 145	0.04	108
^{41}K	1514	0.73	603	2.63	1514	1.85	0.11
^{44}Ca	252	0.21	34	0.27	1189	0.64	0.27
^{49}Ti	242	1.21	319	1.14	215	0.64	0.45
^{55}Mn	730	1.00	220	1.00	820	1.00	0.24
^{54}Fe	2024	0.86	2117	1.64	2320	1.14	0.24
^{63}Cu	17	1.47	22	1.13	20	1.96	0.63
^{66}Zn	19	0.49	23	0.73	27	2.31	1.16
^{85}Rb	269[a]	0.53	164[a]	3.13	242[a]	2.36	0.19
^{88}Sr	395[a]	0.43	29[a]	1.30	138[a]	1.29	0.27
^{90}Zr	58[a]	0.28	54[a]	0.86	35[a]	0.69	1.79
^{137}Ba	71[a]	0.20	14[a]	1.27	35[a]	0.85	0.64

[a] Value not listed in the certification, but determined by ICP-MS.

which are not listed in the certifications, were found in the spectra with well-matched isotope ratios. To prove the existence of these elements in the samples, we have carried out an experiment by dissolving the samples and using an ICP-MS (Agilent 4500) with the standard addition protocol for quantification. The concentrations of these unexpected elemental isotopes are listed in Table 2. Therefore, the instrument has the potential of becoming a useful tool for geological research.

For the Zinc concentrate sample, a typical spectrum is shown in Fig. 3. The major interferences were also at m/z 18 (H_2O^+) and 19 (H_3O^+). The zinc isotope ratios are not in accord with the theoretical isotope ratios due to the high concentration, which causes a pulse "pile-up" in the counter for ^{64}Zn, ^{66}Zn, and ^{68}Zn peaks.

Relative sensitivity coefficients (RSCs) were used to illustrate differences in ion yield and mass bias in the mass spectrometer.[16,17] The elements with appropriate mass number, ionization potential, and concentration were used as the reference element. In a conventional RSC calculation, doubly charged (even triply

**Table 3** RSCs and LODs of all metal elements in Zinc concentrate YSS030-2006 (^{65}Cu as reference element)

Element (isotope used)	Concentration of YSS030-2006/μg g^{-1}	RSC	LODs/μg g^{-1}
^{57}Fe	1824	1.93	0.38
^{65}Cu	5328	1.00	0.59
^{67}Zn	20 590	1.07	0.43
^{75}As	1000	0.10	4.51
^{107}Ag	101	0.20	2.20
^{114}Cd	947	0.12	2.49
^{121}Sb	189	0.49	3.60
^{208}Pb	3982	0.30	1.01

charged) ions are taken into consideration since a large fraction of those peaks are typically present in the spectra.[18] RSCs shown in Tables 2 and 3 were calculated with sums of peak heights of the singly and multiply charged ions, with limits of detection (LODs) also listed.

It can be easily observed in Table 2 that the ions with an m/z smaller than 30 have small RSCs. The non-uniform transmission property of the rf-only hexapole device may be the major factor causing the mass discrimination against light ions. The results in Tables 2 and 3 demonstrate the variations of RSCs for different elements as well as for the same element in the series. The possible reason is the variation of laser irradiance, ion kinetic energy distributions, instrumental stability, and sample homogeneity. These variations are within one order of magnitude, which indicates that LP-TOFMS can be used for direct semi-quantitative analysis.

Conclusion

LP-TOFMS with a collisional cooling system has proved to be a convenient technique for the simultaneous multi-element analysis of geological samples. Currently, the system has a mass resolving power of 5000 and a limit of detection of 10^{-6}–10^{-7} g g^{-1}. If RCSs can reach an approximately even value, and the spectrum contains few minor interferences, standardless

Fig. 3 Mass spectrum of zinc concentrate YSS030-2006.
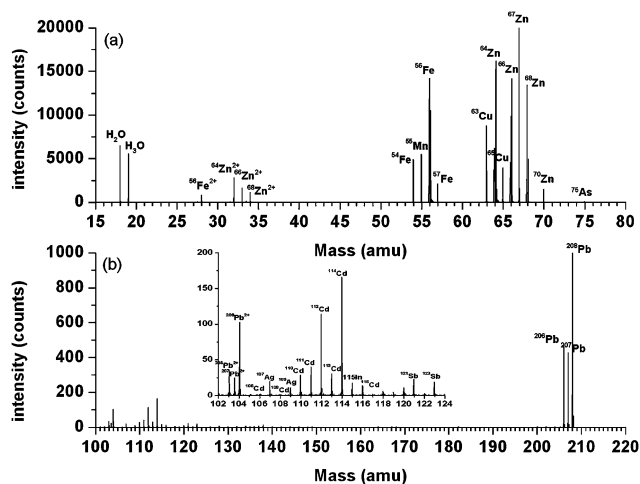
quantitative analysis might be achieved. Other than the operation parameters mentioned previously, the major obstacle for the instrument is the mass bias in the multipole cooling system. Alternative solutions are currently under evaluation to overcome the mass bias problem. Overall, LP-TOFMS has demonstrated features such as conceptual simplicity, ease of operation and less interference than other techniques.

Acknowledgements

References

1 G. Theodoridis and I. N. Papadoyannis, *Mikrochim. Acta*, 2001, **136**, 199–204.
2 D. Günther and B. Hattendorf, *Trends Anal. Chem.*, 2005, **24**, 255–265.
3 J. K. Holt, E. J. Nelson and G. L. Klunder, *J. Phys.: Conf. Ser.*, 2007, **59**, 657–661.
4 K. P. Jochum, B. Stoll, K. Herwig, A. Amini, W. Abouchami and A. W. Hofmann, *Int. J. Mass Spectrom.*, 2005, **242**, 281–289.
5 A. M. Leach and G. M. Hieftje, *Anal. Chem.*, 2001, **73**, 2959–2567.
6 M. Tanner and D. Günther, *Anal. Bioanal. Chem.*, 2008, **391**, 1211–1220.
7 N. I. Ward, S. F. Durrant and A. L. Gray, *J. Anal. At. Spectrom.*, 1992, **7**, 1139–1146.
8 H. R. Kuhn and D. Günther, *Anal. Chem.*, 2003, **75**, 747–753.
9 R. Honig and J. Woolston, *Appl. Phys. Lett.*, 1963, **2**, 138–139.
10 J. S. Becker and H. J. Dietzc, *Fresenius' J. Anal. Chem.*, 1992, **344**, 69–88.
11 E. Denoyer, R. V. Grieken, A.F. and D. F. S. Natusch, *Anal. Chem.*, 1982, **54**, 26.
12 D. Peng, J. He, Q. Yu, L. Z. Chen, W. Hang and B. L. Huang, *Spectrochim. Acta, Part B*, 2008, **63**, 868–874.
13 R. E. Russo, X. L. Mao, H. C. Liu, J. Gonzalez and S. S. Mao, *Talanta*, 2002, **57**, 425–451.
14 K. Niemax, *Fresenius' J. Anal. Chem.*, 2001, **370**, 332–340.
15 W. Hang, *J. Anal. At. Spectrom.*, 2005, **20**, 301–307.
16 A. A. Sysoev and A. A. Sysoev, *Eur. J. Mass Spectrom.*, 2002, **8**, 213–232.
17 J. He, W. W. Zhong, C. Mahan and W. Hang, *Spectrochim. Acta, Part B*, 2005, **61**, 220–224.
18 A. A. Sysoev, S. S. Poteshin, G. B. Kuznetsov, I. A. Kovalev and E. S. Yushkov, *J. Anal. Chem.*, 2002, **57**, 811–820.